Article

Not peer-reviewed version

The Dirac Fermion of a Monopole Pair (MP) Model

Samuel Yuguru *

Posted Date: 13 February 2024

doi: 10.20944/preprints202210.0172.v7

Keywords: dirac fermion; dirac belt-trick; 4D space-time; quantum field theory

 doi:10.20944/preprints202210.0172.v7

Article

The Dirac Fermion of a Monopole Pair (MP) Model

Samuel. P. Yuguru

Department of Chemistry, School of Natural and Physical Sciences, University of Papua New Guinea, P. O. Box 320, Waigani Campus, National Capital District 134, Papua New Guinea; samuel.yuguru@upng.ac.pg; Tel.: +675-326-7102; Fax. : +675-326-0369

Abstract: The electron of spin −1/2 is a Dirac fermion of a complex four-component spinor field. Though it is effectively addressed by relativistic quantum field theory, an intuitive form of the fermion still remains lacking and it is often described by the so-called Dirac belt trick. In this novel undertaking, the fermion is examined within the boundary posed by a recently proposed MP model of a hydrogen atom into 4D space-time. Its physicality and transformation to Dirac fermion of four-component spinor is unveiled consistent with Dirac belt trick. The outcomes are compatible with Dirac field theory and other associated features like, SO(3) group to SU(2) transition, quantized Hamiltonian, non-relativistic wave function and Feynman diagrams. The model though speculative could become important towards defining the fundamental state of matter and its field theory subject to further investigations.

Keywords: dirac fermion; dirac belt-trick; 4D space-time; quantum field theory

1. Introduction

At the fundamental level of matter, particles are described by wave-particle duality, charges and their spin property. These properties are revealed from light interactions and are pursued by the application of relativistic quantum field theory (QFT) [1–2]. The theory of special relativity defines lightspeed, c to be constant in a vacuum and the rest mass of particles to be, $m = E/c^2$ with E as energy. The particle-like property of light waves consists of massless photons possessing spin 1 of neutral charge. Any differences to its spin, charge and mass-energy equivalence provide the inherent properties of particles for the matter at the fundamental level and this is termed causality [3, 4]. Based on QFT, particles appear as excitation of fields permeating space at less than lightspeed. There is a level of indetermination towards unveiling of the charge and spin property, whereas the wave-particle duality is depended on the instrumental set-up [5, 6]. The probability of locating the electron within the atom is defined by non-relativistic Schrödinger's electron field, ψ, and it is not compatible to the excitation of the electromagnetic field for particle manifestation [7]. In other words, it is difficult to imagine wavy form of particles freely permeating space without interactions and this somehow collapses to a point at observation [8].

At the atomic state, the energy is radiated in discrete energy forms in infinitesimal steps of Planck radiation, $\pm h$. The interpretation is consistent with observations except for the resistive nature of proton decay [9]. The preferred quest for particle observation at the atomic level is to make non-relativistic equations become relativistic due to the shared properties of both matter and light at the fundamental level as mentioned above.

Beginning with Klein-Gordon equation [10], the energy and momentum operators of Schrödinger equation,

$$\hat{E} = i\hbar\frac{\partial}{\partial t}, \qquad \hat{p} = -i\hbar\boldsymbol{\nabla}, \tag{1}$$

are adapted in the expression,

$$\left(\hbar^2\frac{\partial^2}{\partial t^2} - c^2\hbar^2\boldsymbol{\nabla}^2 + m^2c^4\right)\psi(t,\bar{x}) = 0. \tag{2}$$

 doi:10.20944/preprints202210.0172.v7

Equation 2 incorporates special relativity, $E^2 = p^2c^2 + m^2c^4$ for mass-energy equivalence, $\boldsymbol{\nabla}$ is the del operator in 3D space, $\hbar$ is reduced Planck constant and i is an imaginary number, $i = \sqrt{-1}$. Only one component is considered in Equation 2 and it does not take into account the negative energy contribution from antimatter. In contrast, the Hamiltonian operator, $\hat{H}$ of Dirac equation [11] for a free particle is,

$$\hat{H}\psi = (-i\boldsymbol{\nabla}.\boldsymbol{a} + m\beta)\psi. \tag{3}$$

The ψ has four-components of fields, i with vectors of momentum,∇ and gamma matrices, α, β represent Pauli matrices and unitarity. The concept is akin to, $e^+ e^- \longrightarrow 2\gamma$, where the electron annihilates with its antimatter to produce two gamma rays. Antimatter existence is observed in Stern-Gerlach experiment and positron from cosmic rays. While the relativistic rest mass is easy to grasp, how fermions acquire mass other than Higgs field remains yet to be solved at a satisfactory level [12]. But perhaps, the most intriguing dilemma is offered by the magnetic spin ±1/2 of the electron and how this translates to a Dirac fermion of four-component spinor field. Such a case remains a very complex topic, whose intuitiveness in terms of a proper physical entity remains lacking and it is often described either by Dirac belt trick [13] or Balinese cup trick [14]. Others relatable descriptions include Klein bottle [15] and Dirac scissors problem [16]. These descriptions dwell on the possible formation of Dirac strings from atom decay. However, suppose the atom is preserved, how the electron can be physically transformed into Dirac fermion is examined within a proposed MP model. Such a process appears compatible with Dirac belt trick, its field theory and other associated features like SO(3) transition to SU(2) symmetry. The model though speculative could become important towards defining the fundamental state of matter and its field theory subject to further investigations.

2. Unveiling Dirac Belt Trick by SO(3) to SU(2) Transition

The electron's orbit of time reversal in discrete continuum form of sinusoidal is defined by Planck radiation, h and is linked to Bohr orbits (BOs) into n-dimensions of energy levels. In forward time, the orbit is transformed into an elliptical shape of a monopole pair (MP) field that undergoes clockwise precession (Figure 1a,b). The torque or right- handedness shifts the electron from positions 0 to 3 to assumed 360° rotation. Maximum twist is attained at the point-boundary or vertex of the MP field at the starting position due to time reversal orbit against clockwise precession. The electron flips to spin down at position 4 to assume an isospin in violation of spherical lightspeed and begins the unfolding process. Another 360° rotation from positions 5 to 8 restores the electron to its original state. These intuitions relate well to Dirac belt trick at 720° rotation assumed at minimal energy of spherical lightspeed in wave-diffraction form. The electron-positron transition at the point-boundary of position 0 promotes radiation, $E = nhv$ from twisting and unfolding process and this somehow sustains the principle axis of the MP field akin to arrow of time in asymmetry. Radiations of Hilbert space with respect to the electron's position translate to Hamiltonian by clockwise precession at spherical lightspeed. The conditions for the inertia frame of reference (Figure 1a) are given by,

$$\lambda_{\pm}^2 = \lambda_{\pm} \quad Tr\lambda_{\pm} = 2\,\lambda_+ + \lambda_- = 1, \tag{4}$$

where the trace function, Tr is the sum of all elements within the model. It can be described in the form,

$$g \in G, \tag{5}$$

where g is the electron's position as subset of the space, G assigned to the spherical model. For the conjugate pairs, 1, 3 and 5, 7, Equation (5) validates the operations,

$$g_{1,5} + g_{3,7} \in G \tag{6a}$$

and

$$g + (-g) = i. \tag{7b}$$

 doi:10.20944/preprints202210.0172.v7

The form, $g_1 + g_3 \neq g_5 + g_7$ due to radiation loss from the electron-positron transition at the point-boundary is assumed along the *z*-axis. By intermittent precession (Figure 1c), the inner product of *r* is generated in the form,

$$\vec{r}_1 \,.\, \vec{r}_2 = |\vec{r}_1 \,||\, \vec{r}_2| cos\theta \tag{7}$$

where rotation of both vectors preserve the lengths and relative angles. By assigning rotation matrix, *R* to Equation (7), its transposition is,

$$(Rr_1)^T (Rr_2) = r_1^T r_2 I, \tag{8}$$

so the identity matrix, $I = R^T \times R$. The orthogonal relationship by clockwise precession of the model at 90° for all rotations suggests, $R \in$ SO(3). The general rotations of SO(3) group in 3D is,

$$G_u(g_\theta) = \begin{pmatrix} 1 & 0 & 0 \\ 0 & cos\theta & -sin\theta \\ 0 & sin\theta & cos\theta \end{pmatrix} \begin{pmatrix} x \\ y \\ z \end{pmatrix}. \tag{9}$$

When rotating as 2 x 2 Pauli vector for SU(2) symmetry with respect to a light-cone (Figure 1d), Equation (9) translates to the form,

$$\pm \begin{pmatrix} cos\frac{\theta}{2} & isin\frac{\theta}{2} \\ isin\frac{\theta}{2} & cos\frac{\theta}{2} \end{pmatrix} = \begin{pmatrix} z & x - y_i \\ x + y_i & -z \end{pmatrix} = \begin{vmatrix} \xi_1 \\ \xi_2 \end{vmatrix} |-\xi_2 \quad \xi_1|, \tag{10}$$

where ξ_1 and ξ_2 are Pauli spinors with respect to conjugate pairs of positions, 1, 3 and 5,7. These are of rank 1 to rank 1/2 tensor relevant for Dirac matrices. Changes in *z*-axis by precession is trivial for amplitude projection along the *x*-*y* plane (Figure 1d). Similar relationships can be pursued for $G(g_\phi)$ with respect to the BO (Figure 1d) in the form,

$$G_u(g_\phi) = \begin{pmatrix} cos\phi & -sin\phi & 0 \\ sin\phi & cos\phi & 0 \\ 0 & 0 & 1 \end{pmatrix} \begin{pmatrix} x \\ y \\ z \end{pmatrix} = \pm \begin{pmatrix} e^{i\frac{\phi}{2}} & 0 \\ 0 & e^{-i\frac{\phi}{2}} \end{pmatrix}. \tag{11}$$

Substitution of Equation (11) to accommodate the qubits -1, 1 and 0 at the point-boundary by polarization due to the electron-positron transitoin (Figure 1c) is relevant to the Lie group such as,

$$e^\theta \begin{bmatrix} 0 & -1 & 0 \\ 1 & 0 & 0 \\ 0 & 0 & 0 \end{bmatrix} = \begin{bmatrix} cos\theta & -sin\theta & 0 \\ sin\theta & cos\theta & 0 \\ 0 & 0 & 1 \end{bmatrix}. \tag{12}$$

Equations (4) to (12) offer some useful insights to the pursuit of QFT for the Dirac spinor when applied within the dynamics of the MP model. How these explanations could align with Dirac theory and its related components are further explored.

Preprints.org (www.preprints.org) | NOT PEER-REVIEWED | Posted: 13 February 2024 doi:10.20944/preprints202210.0172.v7

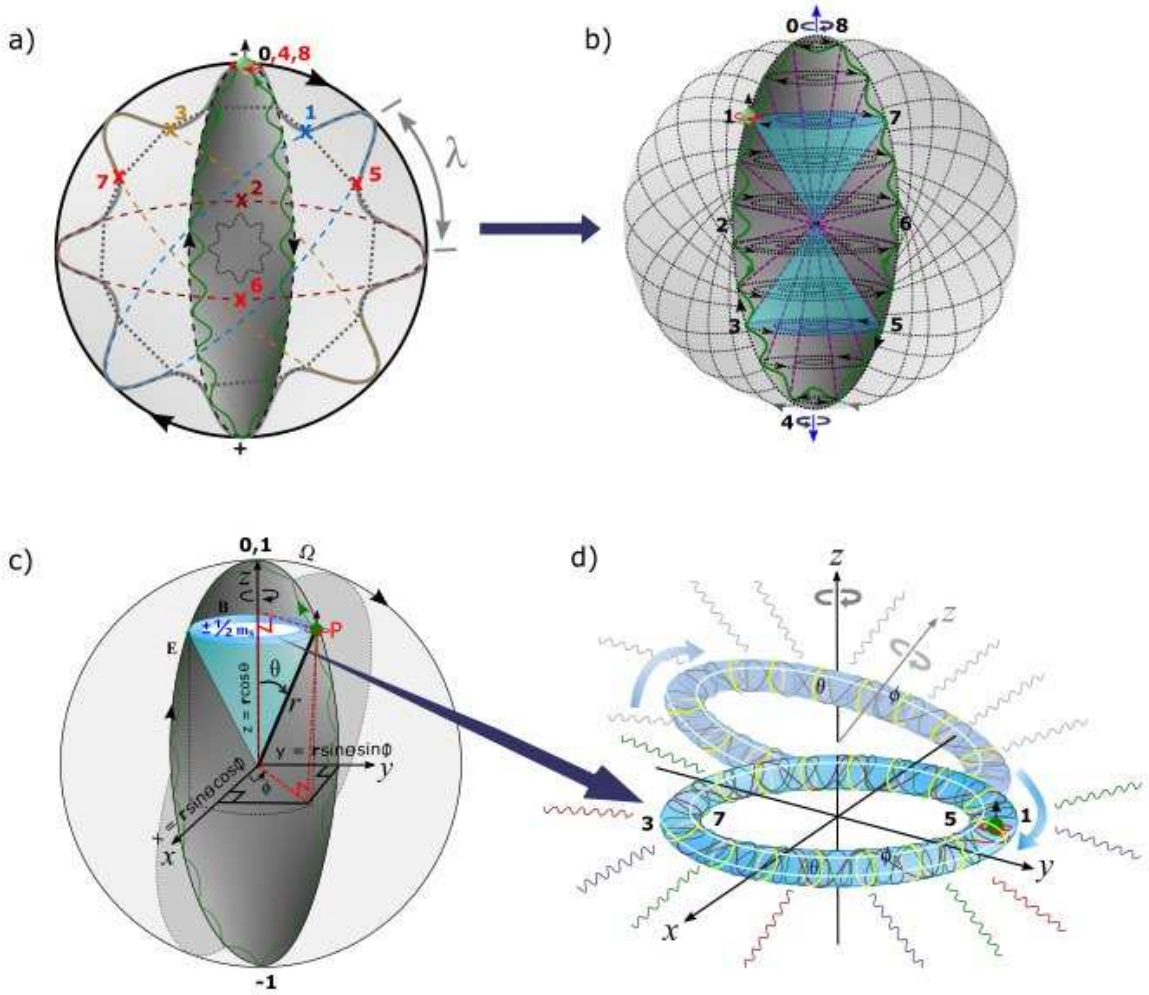

Figure 1. The MP model [17]. (a) In flat space, a spinning electron (green dot) in orbit of sinusoidal form (green curve) is of time reversal. It is normalized to an elliptical MP field (black area) of a magnetic field, **B** by clockwise precession (black arrows), and this generates a circular electric field, **E** of inertia frame, λ. The shift in the electron's position from positions 0 to 4 at 360° rotation against clockwise precession generates maximum twist. At position 4, the electron flips to a positron to begin the unfolding process from positions 5 to 8 for another 360° rotation to restore the electron to its original state analogous to Dirac belt trick. For the total of 720° rotation, a dipole moment (±) is generated for the classical spherical model. (b) The BOs defined by conjugate numbered pairs, 1,3 and 5,7 translate to angular momentum (purple dotted lines) of spin ±1/2 depicted by a pair of light cones (navy colored) in Minkowski space-time. These are projected in degeneracy toward singularity at the center. (c) SO(3) group of 3-manifolds. The spinning principle axis of the MP field allows for twisting of the elliptical field to transform it to 3D space, where conjugate pairs of 1, 3 and 5, 7 form a topological torus of a pair of light cones projected towards the center at spherical lightspeed. These are applicable to SU(2) symmetry in degeneracy and somewhat sustains Pauli exclusion principle of spin ± 1/2. The transformation by precession, Ω polarizes the model to generate qubits, 0 and ±1 at spherical lightspeed. The polar coordinates (r, θ, Φ) are attributed to non-relativistic Schrödinger wave function with respect to the electron's position in space. (d) Topological torus emerges from BOs defined by ϕ (white loops) and their dissection perpendicularly by θ (yellow circles) due to intermittent clockwise precession. All light-matter interactions are normalized to the electron's position within the torus as the base point in Hilbert space. Any translation along *z*-axis for the BO in degeneracy equates to Fourier transform into linear time.

Preprints.org (www.preprints.org) | NOT PEER-REVIEWED | Posted: 13 February 2024 doi:10.20944/preprints202210.0172.v7

3. Dirac Field Theory and Its Related Components

The descriptions of Dirac fermion based on the MP model are applicable for the pursuit of Dirac theory and its related components. In this section certain components of the field theory and its related features [1, 2, 10, 11] are explored in bullet points for their relevance to this undertaking.

⇒ **Dirac theory and helical property.** Based on the MP model (e.g., Figure 1a), further demonstrations on Dirac belt-trick with respect to twisting and unfolding process of the electron's elliptical orbit when subjected to clockwise precession are presented in Figure 2a–f. The fermion field is defined by the famous Dirac equation of the generic form,

$$i\hbar\gamma^u\partial_u\psi(x) - mc\psi(x) = 0, \tag{13}$$

where γ^u are gamma matrices. The exponentials of the matrices, $\{\gamma^o\gamma^1\gamma^2\gamma^3\}$ are attributed to the electron's position by clockwise precession acting on its orbit.

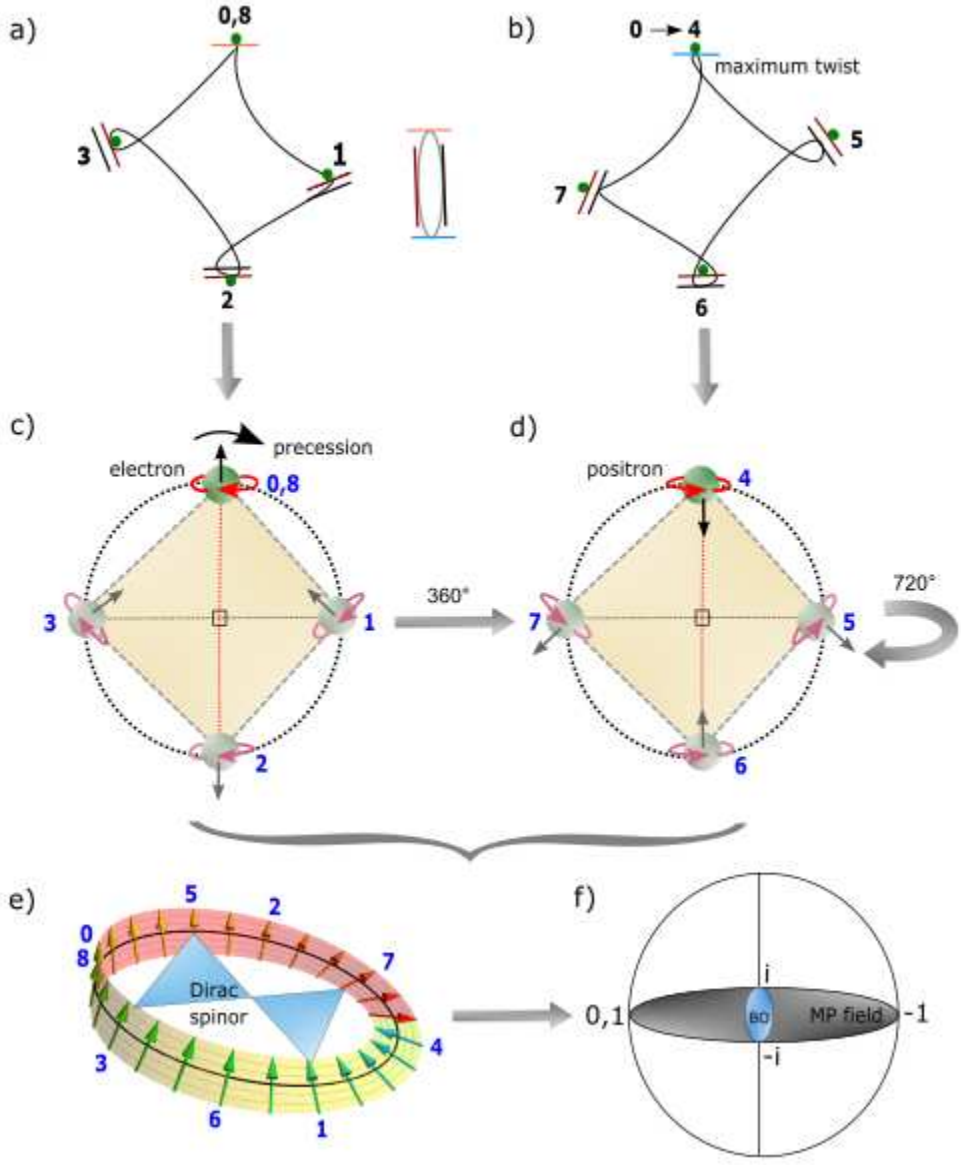

Figure 2. Dirac belt trick. (a) The electron (green dot) induced rotation due to clockwise precession against its time reversal elliptical orbit insinuates a close loop. The position of the particle on a straight path (colored lines) is referenced to the MP field of elliptical shape (centered image) based on the MP model (Figure 1a). The loop of spin 1/2 is confined to a hemisphere and is formed at spherical lightspeed. (b) Maximum twist is attained at position 4 as detectable energy and the unfolding process offers another loop at 360° rotation for a total of 720° rotation to restore the electron at position 8 or 0 akin to Dirac belt trick. (c) Precession normalizes the loop to generate an electron of positive helicity

 doi:10.20944/preprints202210.0172.v7

or right-handedness. The spin up vector correlates with the direction of precession. (d) The electron flips to a positron of negative helicity or left-handedness. The spin down vector is in opposite direction to the direction of precession to begin the unfolding process. (e) Dirac spinor at spherical lightspeed combines positions 0 → 8 of superposition state. The tilt in position 4 compared to position 0 is attributed to energy loss from the electron-positron transition in the form, $E = h\nu = g\beta B$. The emergence of the pair of light-cones are attributed to positions 1, 3 and 5, 7 of hermitian conjugates. (f) Polarization of the model either horizontal or vertical with respect to the electron-positron pair, ±i generates qubits 0 and ±1 at positions, 0, 4 and 8 (see also Figure 1a). Image (e) adapted from ref. [18].

For example, $\gamma^o$is assigned to the vertex of the MP field and by electron-positron transition, it sustains *z*-axis or arrow of time in asymmetry at position 0. The $\gamma^1\gamma^2\gamma^3$ variables of Dirac matrices are relatable to the electron shift in its positions. Orthogonal projections of the space-time variables, $\frac{1}{2}(1 \pm i\gamma^0\gamma^1\gamma^2\gamma^3)$ are confined to a hemisphere and assigned to a light cone (e.g., Figure 1c). These are incorporated into the famous Dirac equation,

$$\left(i\gamma^0\frac{\partial}{\partial t} + cA\frac{\partial}{\partial x} + cB\frac{\partial}{\partial y} + cC\frac{\partial}{\partial z} - \frac{mc^2}{\hbar}\right)\psi(t,\vec{x}), \tag{14}$$

where *c* acts on the coefficients A, B and C and transforms them to γ^1, γ^2 and γ^3. The exponentials of γ are denoted *i* for off-diagonal Pauli matrices for the light-cone (Figure 1d) and is defined by,

$$\gamma^i = \begin{pmatrix} 0 & \sigma^i \\ -\sigma^i & 0 \end{pmatrix}, \tag{15a}$$

and zero exponential, γ^o is,

$$\gamma^0 = \begin{pmatrix} 0 & 1 \\ 1 & 0 \end{pmatrix}. \tag{16b}$$

σ^i is relevant to oscillations assumed at the BOs (Figure 1d) with anticommutation relationship, $e^+(\psi) \neq e^-(\bar{\psi})$ of chiral symmetry (Figure 2c and 2d). The associated vector gauge invariance exhibits the following relationships,

$$\psi_L \rightarrow e^{i\theta L}\psi_L \tag{17}$$

or

$$\psi_R \rightarrow e^{i\theta L}\psi_R. \tag{18}$$

The exponential factor, $i\theta$ refers to the position, *i* of the electron of a complex number and θ, is its angular momentum (e.g., Figure 1c). The unitary rotations of right-handedness (*R*) or positive helicity and left-handedness (*L*) or negative helicity are applicable to the electron transformation to Dirac fermion (Figure 2a). The process is confined to a hemisphere and this equates to spin 1/2 property of a complex spinor (Figure 2b). Two successive rotations of the electron in orbit equal to clockwise precession of the MP field is identified by $i\hbar$. The chirality or vector axial current at the point-boundary is assigned to polarization, ±1 of the model (Figure 1c). The helical symmetry from projections operators or isospin acting on the spinors (Figure 2e) is,

$$P_L = \frac{1}{2}(1 - \gamma_5) \tag{19}$$

and

$$P_R = \frac{1}{2}(1 - \gamma_5). \tag{17b}$$

Dirac matrices of eigenstates, γ_5 at fixed momentum is attributed to the BOs. The usual properties of projection operators are: $L + R = 1$; $RL = LR = 0$; $L^2 = L$ and $R^2 = R$ (e.g., Figure 2a–d).

 doi:10.20944/preprints202210.0172.v7

⇒ **Quantized Hamiltonian.** Dirac fermion or spinor is denoted $\psi(\mathbf{x})$ in 3D Euclidean space and it is superimposed onto the MP model of 4D space-time, $\psi(\mathbf{x},t)$ due to clockwise precession (Figure 1a and 1b). The model into Minkowski space-time resembles Poincaré sphere (Figure 3a). The Dirac four-component spinor, $\psi = \begin{pmatrix} \psi_0 \\ \psi_1 \\ \psi_2 \\ \psi_3 \end{pmatrix}$ is attributed to positions 1,3 and 5, 7 of hermitian conjugate pairs in 3D space (Figure 1a). Dirac spinor on the surface of Poincaré sphere can relate to both positive and negative curvatures of non-Euclidean space (e.g., Figure 2a and 2b). Convergence of positions 1 and 3 at either position 0 or 2 is relevant to the equivalence principle based on general relativity. The straight paths of the Dirac spinor (Figure 2c and 2d) define Euclidean space. Any light paths tangential to the point-boundary is expected to transform the spinor into linear time akin to Fourier transform and thus, induce wave function collapse (Figure 3b). The probabilistic outcome of the spin is given by Born's rule,$|\psi|^2$. The past or future events of the electron path from positions 0 to 8 are not accounted for at observation. The shift in the electron's position of hermitian conjugates (e.g., Figure 2c and 2d), $P(0\rightarrow 8) = \int_\tau \psi^* \hat{H} \psi d\tau$ assumes Hamiltonian space by precession with τ equal to arrow of time along z-axis (Figure 1d). Unitarity by Euler's formula, $e^{i\pi} + 1 = 0$ is preserved in real space (e.g., Figure 1c).

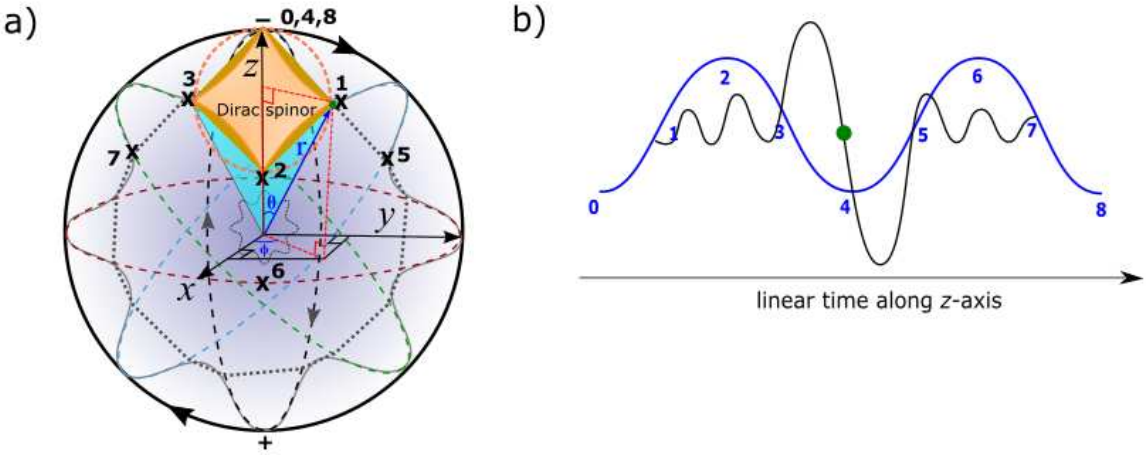

Figure 3. Dirac spinor and observation. (a) The spinor is superimposed on Poincaré sphere and it consists of both Euclidean (straight paths) and non-Euclidean (negative and positive curves) spaces. Clockwise precession by geodesic motion induces a circle at 360° rotation to the negative curves at positions 0 to 3. The polar coordinates (r, θ, Φ) are linked to a light cone (navy colored) similar to Figure 1c. (b) By Fourier transform, both radial (blue wavy curve) and angular (black wavy curve) wave functions are incorporated into linear time and the process mimics somehow mimics wave function collapse (see also Figure 1d).

Two ansatzes adapted from Equation (13) are given by,

$$\psi = u(\mathbf{p})e^{-ip.x}, \tag{18a}$$

and

$$\psi = v(\mathbf{p})e^{ip.x}. \tag{18b}$$

By linear transformation, the hermitian plane wave solutions form the basis for Fourier components in 3D space (Figures 1d and 3b). Decomposition of quantized Hamiltonian ensues as,

 doi:10.20944/preprints202210.0172.v7

$$\psi(x) = \frac{1}{(2\pi)^{3/2}} \int \frac{d^3}{2E_{\mathbf{p}}} \sum_s \left(a_{\mathbf{p}}^s u^s(p) e^{-ip.x} + b_{\mathbf{p}}^{s\dagger} v^s(p) e^{ip.x} \right), \tag{19a}$$

and its conjugate form by,

$$\bar{\psi}(x) = \frac{1}{(2\pi)^{3/2}} \int \frac{d^3}{2E_{\mathbf{p}}} \sum_s \left(a_{\mathbf{p}}^{s\dagger} \bar{u}^s(p) e^{ip.x} + b_{\mathbf{p}}^s \bar{v}^s(p) e^{-ip.x} \right). \tag{19b}$$

The coefficients $a_{\mathbf{p}}^s$ and $a_{\mathbf{p}}^{s\dagger}$ are ladder operators for u-type spinor and $b_{\mathbf{p}}^s$ and $b_{\mathbf{p}}^{s\dagger}$ for v-type spinor. These are applicable to Dirac spinors of two spin states, ±1/2 and $\bar{v}^s$ and $\bar{u}^s$ as their antiparticles (Figure 2a and 2b). The operators are applicable to BOs into n-dimensions for the production of complex fermions, ±1/2, ±3/2, ±5/2 and so forth (Figures 1d and 4a). Dirac Hamiltonian of one-particle quantum mechanics relevant to the MP model of hydrogen atom type is,

$$H = \int d^3x \psi^\dagger(x) [-i\gamma^0 \gamma . \boldsymbol{\nabla} + m\gamma^0] \psi(x). \tag{20}$$

The quantity in the bracket is provided in Equation (3). By parity transformation, the observable and holographic oscillators are canonically conjugates (Figure 4b). The associated momentum is,

$$\pi = \frac{\partial \mathcal{L}}{\partial \psi} - \bar{\psi} i\gamma^0 = i\psi^\dagger. \tag{21}$$

With z-axis of the MP field aligned to the vertex in asymmetry (Figure 1c), the V-A currents comparable to Fourier transform are projected in either x or y directions in 3D space (Figures 1d and 3b). These assume the relationships,

$$\left[\psi_\alpha(\mathbf{x}, t), \psi_\beta(\mathbf{y}, t) \right] = \left[\psi_\alpha^\dagger(\mathbf{x}, t), \psi_\beta^\dagger(\mathbf{y}, t) \right] = 0, \tag{22a}$$

and its matrix form,

$$\left[\psi_\alpha(\mathbf{x}, t), \psi_\beta^\dagger(\mathbf{y}, t) \right] = \delta_{\alpha\beta} \delta^3(\mathbf{x} - \mathbf{y}), \tag{23}$$

where α and β denote the spinor components of ψ. Equations (22a) refers to unitarity of the model and Equation (22b) is assumed by electron-positron transition at the point-boundary (Figure 2b). The ψ independent of time in 3D space obeys the uncertainty principle with respect to the electron's position, $\mathbf{p}$ and momentum, $\mathbf{q}$, as conjugate operators (Figure 1c). The commutation relationship of $\mathbf{p}$ and $\mathbf{q}$ obeys the relationship,

$$\left\{ a_{\mathbf{p}}^r, a_{\mathbf{q}}^{s\dagger} \right\} = \left\{ b_{\mathbf{p}}^r, b_{\mathbf{q}}^{s\dagger} \right\} = (2\pi)^3 \delta^{rs} \delta^3(\mathbf{p} - \mathbf{q}). \tag{23}$$

Equation (23) incorporates both matter and antimatter and their translation to linear time (Figure 3b). The electron as a physical entity generates a positive-frequency such as,

$$\langle 0 | \psi(x) \bar{\psi}(y) | 0 \rangle = \langle 0 | \int \frac{d^3p}{(2\pi)^3} \frac{1}{\sqrt{2E_{\mathrm{p}}}} \sum_r a_{\mathrm{p}}^r u^r(p) e^{-ipx} \times \int \frac{d^3q}{(2\pi)^3} \frac{1}{\sqrt{2E_{\mathrm{q}}}} \sum_s a_{\mathrm{q}}^{s\dagger} \bar{u}^s(q) e^{iqy} \; | 0 \rangle. \tag{24}$$

 doi:10.20944/preprints202210.0172.v7

Equation (24) could explain the dominance of matter (electron) over antimatter if the latter is accorded to the conceptualization process of Dirac fermion provided by the model (e.g., Figure 2a and 2b).

⇒ **Non-relativistic wave function.** Observation by light-matter interaction allows for the emergence of the model from the point-boundary at Planck length. Subsequent energy shells of BOs at the n-levels by excitation accommodates complex fermions, ±1/2, ±3/2, ±5/2 and so forth (Figure 4a). The orbitals of 3D are defined by total angular momentum, $\vec{J} = \vec{l} + \vec{s}$ and this incorporates both orbital angular momentum, l and spin, s. Within a hemisphere, the model is transformed to a classical oscillator. By clockwise precession, a holographic oscillator from the other hemisphere of the MP field remains hidden. One oscillator levitates about the other (Figure 4b) and both are not simultaneously accessible to observation in linear time by Fourier transform (e.g., Figure 3b). The n-levels for the fermions can be pursued for Fermi-Dirac statistics with the point-boundary assigned to zero-point energy (ZPE). For $\pm\vec{J}$ splitting (Figure 4a), this can apply to Landé interval rule due to the electron isospin and somehow it can accommodate lamb shift and thus, hyperfine structure constant. Such a scenario is similar to how vibrational spectra of a harmonic oscillator for diatoms like hydrogen molecule incorporates rotational energy levels. The difference of the classical oscillator to the quantum scale is the application of Schrödinger wave equation (e.g., Figure 4a).

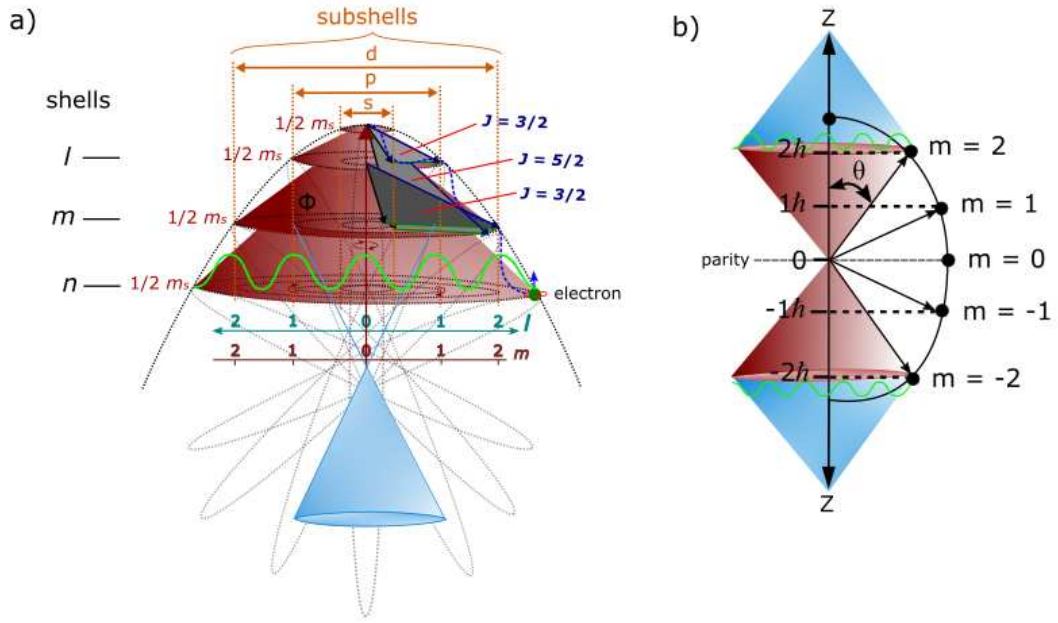

Figure 4. Light-MP model coupling. (a) To an external observer, the topological point-boundary provides the origin for the emergence of the oscillator, $J_z = S + L$ (maroon light cones). Increase into n-dimensions, k to l offers asymptotic boundary to the energy shells and subshells inclusive of the hidden oscillator. The BOs in degeneracy, Φ_i (see also Figure 1d) at the n-levels of the observable oscillator can accommodate Fermi-Dirac statistics (green wavy curve) and possibly Fock space for non-relativistic many-particle systems if mulielectron are assigned to multiple MP fields. The observable oscillator is partitioned at the infinite boundary at the center of the MP field and is equivalent to classical limit of the holographic oscillator. The blue light cone is from the perspective of the observer at the center. (b) The emergence of quantized magnetic moment, $\pm J_z = m_j\hbar$ from the point-boundary (maroon light cones) levitates about the internal frame of the model (blue light cones). Parity transformation for the conjugate pairs is confined to a hemisphere (e.g., Figure 2a and 2b). Scatterings (green wavy curves) are applicable to light-MP model interactions along the BOs (see also Figure 1d).

Preprints.org (www.preprints.org) | NOT PEER-REVIEWED | Posted: 13 February 2024 doi:10.20944/preprints202210.0172.v7

⇒ **Weyl spinor.** The light cone from the point-boundary within a hemisphere accommodates both matter and antimatter by parity transformation to generate Dirac spinor (Figures 1c, 2a–d and 4b). It is described in the form,

$$\psi = \begin{pmatrix} \psi_0 \\ \psi_1 \\ \psi_2 \\ \psi_3 \end{pmatrix} = \begin{pmatrix} \psi_1 \\ \psi_3 \\ \psi_5 \\ \psi_7 \end{pmatrix}. \tag{25}$$

Equation (25) corresponds to spin up fermion, a spin down fermion, a spin up antifermion and a spin down antifermion. These are relevant to the electron's shift in positions of conjugate pairs (e.g., Figure 2c and 2d). By forming its own antimatter within a light cone in a hemisphere (Figure 4b), the Dirac fermion somewhat resembles Majorana fermions. It is difficult to observe them due to the wave function collapse long *z*-axis of linear time (e.g., Figure 3b). Non-relativistic Weyl spinor of a pair of light cones relevant to Schrödinger wave equation are of holographic type (Figure 4a and 4b). These are defined by reduction of Equation (25) to bispinor of the form,

$$\psi = \begin{pmatrix} u_+ \\ u_- \end{pmatrix}, \tag{26}$$

where $u_\pm$ are Weyl spinors of chirality due to the electron position as a physical entity. By parity operation, $x \rightarrow x' = (t, -\mathbf{x})$, qubits 1 and −1 are generated at the vertices of the MP field (e.g., Figure 1c). Depending on the reference point-boundary of the BO (Figure 1d), the exchanges of left- and right-handed Weyl spinor assumed the process,

$$\begin{pmatrix} \psi'_L \\ \psi'_R \end{pmatrix} = \begin{pmatrix} \psi_R(x) \\ \psi_L(x) \end{pmatrix} \Rightarrow \begin{matrix} \psi'(x') = \gamma^0 \psi(x) \\ \bar{\psi}'(x') = \bar{\psi}(x)\gamma^0. \end{matrix} \tag{27}$$

Conversion of Weyl spinors of 4D space-time to Dirac bispinor, $\xi^1\ \xi^2$ of 3D space are expected diagonally at positions 1 and 3 along BO (Figure 1d). Comparably, the two-component spinor, $\xi^1\ \xi^2 = 1$ are normalized at the point-boundaries with the electron as the base point.

⇒ **Lorentz transformation.** The Hermitian pair, $\psi^\dagger\psi$ of Dirac fermion based on Equation (26) undergo Lorentz transformation in the form,

$$\begin{aligned} u^\dagger u &= (\xi^\dagger\sqrt{p.\sigma},\ \xi\sqrt{p.\bar{\sigma}}\,.\begin{pmatrix} \sqrt{p.\sigma}\xi \\ \sqrt{p.\bar{\sigma}}\xi \end{pmatrix}, \\ &= 2\mathrm{E_P}\xi^\dagger\xi\,. \end{aligned} \tag{28}$$

Equation (28) basically relates to the transformation of the model of 4D space-time to linear time at observation comparable to Fourier transform (e.g., Figure 3b). The corresponding Lorentz scalar applicable to scattering at the BOs (Figure 1d) is,

$$\bar{u}(p) = u^\dagger(p)\gamma^0. \tag{29}$$

Equation (29) is referenced to *z*-axis as the principle axis of the MP field of a dipole moment in asymmetry (Figure 1c). By identical calculation to Equation (28), the Weyl spinor becomes,

$$\bar{u}u = 2m\xi^\dagger\xi, \tag{30}$$

with respect to the light-cone (Figure 4a). It is difficult to distinguish Weyl spinor and Majorana fermion from Dirac spinor by observations due to superposition of electron-positron pairings (e.g., Figure 2e) but somehow their distinctions are viable within the MP model.

Preprints.org (www.preprints.org) | NOT PEER-REVIEWED | Posted: 13 February 2024 doi:10.20944/preprints202210.0172.v7

⇒ **Feynman diagrams.** The two types of particles pursued by Dirac field theory consist of bosons and fermions. The former of whole integer spin 0 and 1 vectors are force-carrying particles and the latter of spin 1/2 are fundamental building blocks of matter. Within the prospects of the MP model, both spin 1 and 0 are attributed to the point-boundary of ZPE of a classical oscillator (Figure 4a). By conservation of the model, ejection of the electron (object) would permit the emergence of particle-hole of isospin. Its constriction at high energy can somewhat mimic Higgs boson at the point-boundary and by relaxation translate to boson types, Z^0 to $W^{\pm}$ based on mass-energy differences from, $m = 0$ to $m > 0$. Ejection of an electron (or positron) by beta decay, $\beta^{\pm}$ would insinuate neutrino types of helical property without requiring change of color charges by exchange of gluons from up and down quarks (Figure 5b). In this case, the vertices of the MP models along the z-axis would assume center of mass (COM) and the particle-hole may constitute violation of charge conjugation, parity and time reversal symmetry. Any scatterings along the BOs of unidirectional (e.g., Figure 1d) would mimic electron-positron pair as the base point and this can accommodate the fine-structure constant, $a = \frac{e^2}{\hbar c} = \frac{e^2}{4\pi} \approx \frac{1}{137}$ at high energy with $c = \hbar = 1$. The interactions between incoming and outgoing particles of Feynman diagrams (Figure 5a and 5b) obey Einstein mass-energy equivalence in the form,

$$E^2 - |\vec{p}|^2 c^2 = m^2 c^2. \tag{31}$$

Photons bombardment of the model would acquire mass, γ or $\frac{-ig_{uv}}{p^2}$ by on-shell momentum ($p^2 = m^2$) of the BO with respect to the particle's position (Figure 4a) and these are normalized to z-axis of linear time that dissects the vertices, $ie\gamma^u$, $ie\gamma^v$ of the MP field as COM comparable to Fourier transform (Figure 3b). Such interpretations can accommodate any deviations in the anomalous magnetic moment of the electron or particle-hole with respect to variations in the value of a such as for the lamb shift.

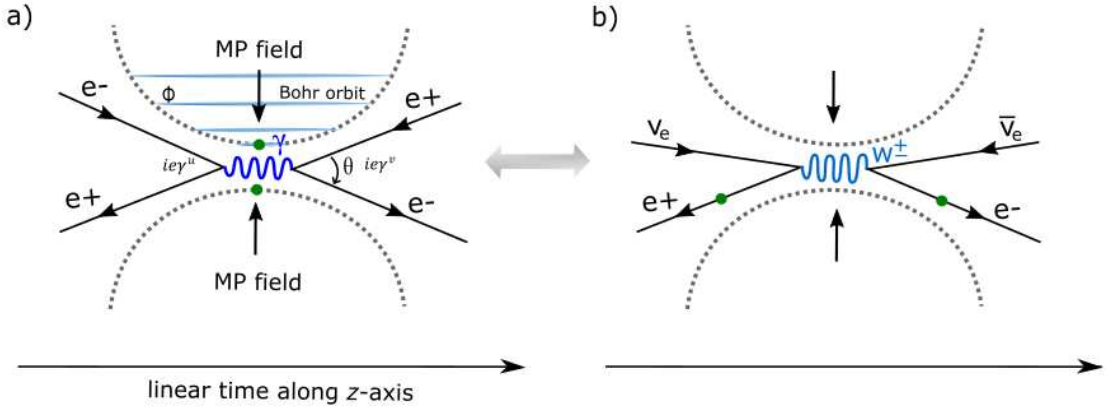

Figure 5. Feynman diagrams for MP models coupling. a) Two electrons, each at a vertex of a MP model may undergo either repulsion or attraction when approaching each other. Symmetry is sustained when secondary photons mimic the COM for the electron-positron transition along the z-axis akin to Fourier transform (Figure 3b). b) Actual ejection of the electron/positron would induce particle-hole isospin. Particle-hole interactions at ZPE can generate various boson types including neutrinos and antineutrinos of helical property mimicking the electron-positron pair (e.g., Figure 2c and 2d). These are relevant to both positive beta (+) and negative beta (-) decays without requiring change in color charges of up and down quarks.

 doi:10.20944/preprints202210.0172.v7

⇒ **Further undertakings.** The relevant themes offered for Dirac field theory with respect to the MP model can be pursued into more depth in quantum electrodynamics and the Standard Model of particle physics. These would include energy-momentum tensor, Fermi-Dirac statistics, Bose-Einstein statistics, causality, Feynman propagator, charge conjugate-parity-time symmetry and so forth.

4. Conclusions

The dynamics of the MP model of 4D space-time offered in this study allows for the transformation of the electron of hydrogen atom type to Dirac fermion of a complex four-component spinor. These demonstrations are compatible with Dirac belt trick, its field theory and other related themes like SO(3) to SU(2) transition. In here, the probable paths to more complex themes of QFT are provided based on the model. Such an intuitive tool can justify the removal of infinite terms during renormalization process and it can be explored for fermions and bosons of both strong and weak nuclear forces. Though the model still remains somewhat speculative, it can become important towards defining the fundamental state of matter and its field theory subject to further investigations.

Data Availability Statement: The modeling data attempted for the current study are available from the corresponding author upon reasonable request.

Competing Financial Interests: The author declares no competing financial interests.

References

1. Peskin, M. E. & Schroeder, D. V. *An introduction to quantum field theory*. Addison-Wesley, Massachusetts, USA (1995). pp 13–25, 40–62.
2. Alvarez-Gaumé, L. & Vazquez-Mozo, M. A. Introductory lectures on quantum field theory. *arXiv preprint hep-th/0510040* (2005).
3. Pawłowski, M. et al. Information causality as a physical principle. *Nature* **461**(7267), 1101-1104 (2009).
4. Henson, J. Comparing causality principles. *Stud. Hist. Philos M. P*, **36**(3), 519-543 (2005).
5. Li, Z. Y. Elementary analysis of interferometers for wave—particle duality test and the prospect of going beyond the complementarity principle. *Chin. Phys. B* **23**(11), 110309 (2014).
6. Rabinowitz, M. Examination of wave-particle duality via two-slit interference. *Mod. Phys. Lett. B* **9**(13), 763-789 (1995).
7. Nelson, E. Derivation of the Schrödinger equation from Newtonian mechanics. *Phys. Rev.* **150**(4), 1079 (1966).
8. Rovelli, C. Space is blue and birds fly through it. *Philos. Trans. Royal Soc. Proc. Math. Phys. Eng.* **376**(2123), 20170312 (2018).
9. Perkins, D. H. Proton decay experiments. *Ann. Rev. Nucl. Part. Sci.* **34**(1), 1-50 (1984).
10. Sun, H. Solutions of nonrelativistic Schrödinger equation from relativistic Klein–Gordon equation. *Phys. Lett. A* **374**(2), 116-122 (2009).
11. Oshima, S., Kanemaki, S. & Fujita, T. Problems of Real Scalar Klein-Gordon Field. *arXiv preprint hep-th/0512156* (2005).
12. Bass, S. D., De Roeck, A. & Kado, M. The Higgs boson implications and prospects for future discoveries. *Nat. Rev. Phys.* **3**(9), 608-624 (2021).
13. Weiss, L. S. et al. Controlled creation of a singular spinor vortex by circumventing the Dirac belt trick. *Nat. Commun.* **10**(1), 1-8 (2019).
14. Silagadze, Z. K. Mirror objects in the solar system?. *arXiv preprint astro-ph/0110161* (2001).
15. Franzoni, G. The klein bottle: Variations on a theme. *Notices of the Am. Math. Soc.* **59**(8), 1094-1099 (2012).
16. Rieflin, E. Some mechanisms related to Dirac's strings. *Am. J. Phys.* **47**(4), 379-380 (1979).
17. Yuguru, S. P. Unconventional reconciliation path for quantum mechanics and general relativity. *IET Quant. Comm.* **3**(2), 99–111 (2022).
18. https://en.wikipedia.org/wiki/Spinor (Retrieved 30 January 2024).